

# **INFLUENCE OF ELECTRON-ELECTRON COLLISIONS ON ELECTRON ENERGY DISTRIBUTIONS AND TRANSPORT IN INDUCTIVELY COUPLED PLASMAS\***

**Alex V. Vasenkov and Mark J. Kushner  
University of Illinois  
Department of Electrical and Computer Engineering  
Urbana, IL 61801**

**E-mail: [vasenkov@uiuc.edu](mailto:vasenkov@uiuc.edu)  
[mjk@uiuc.edu](mailto:mjk@uiuc.edu)**

**URL: <http://uigelz.ece.uiuc.edu>**

**May 2002**

**\*Work supported by CFD Research Corp., NSF,  
Applied Materials, Inc. and the SRC**

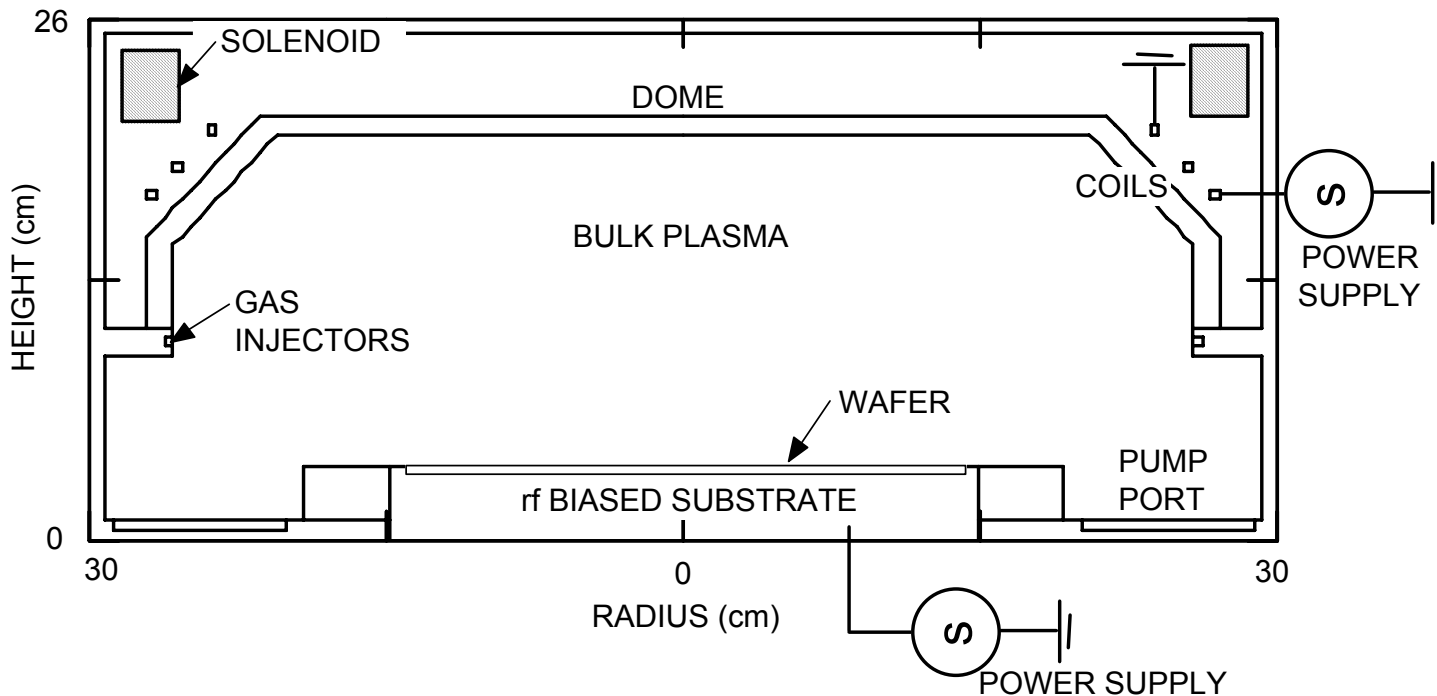
# AGENDA

---

- **Modeling of non-local electron kinetics in ICPs**
- **Description of the model**
- **Validation of the model for ICPs in Ar**
- **Stochastic heating in ICPs**
- **Modeling of electron transport for ICPs in CF<sub>4</sub>**
- **Summary**

# ELECTRON KINETICS IN ICPs

- The trend towards using high-plasma density ( $>10^{11}\text{cm}^{-3}$ ), low gas pressure ( $< 10\text{s mTorr}$ ) sources in materials processing has resulted in renewed interest in electron kinetics in ICPs.



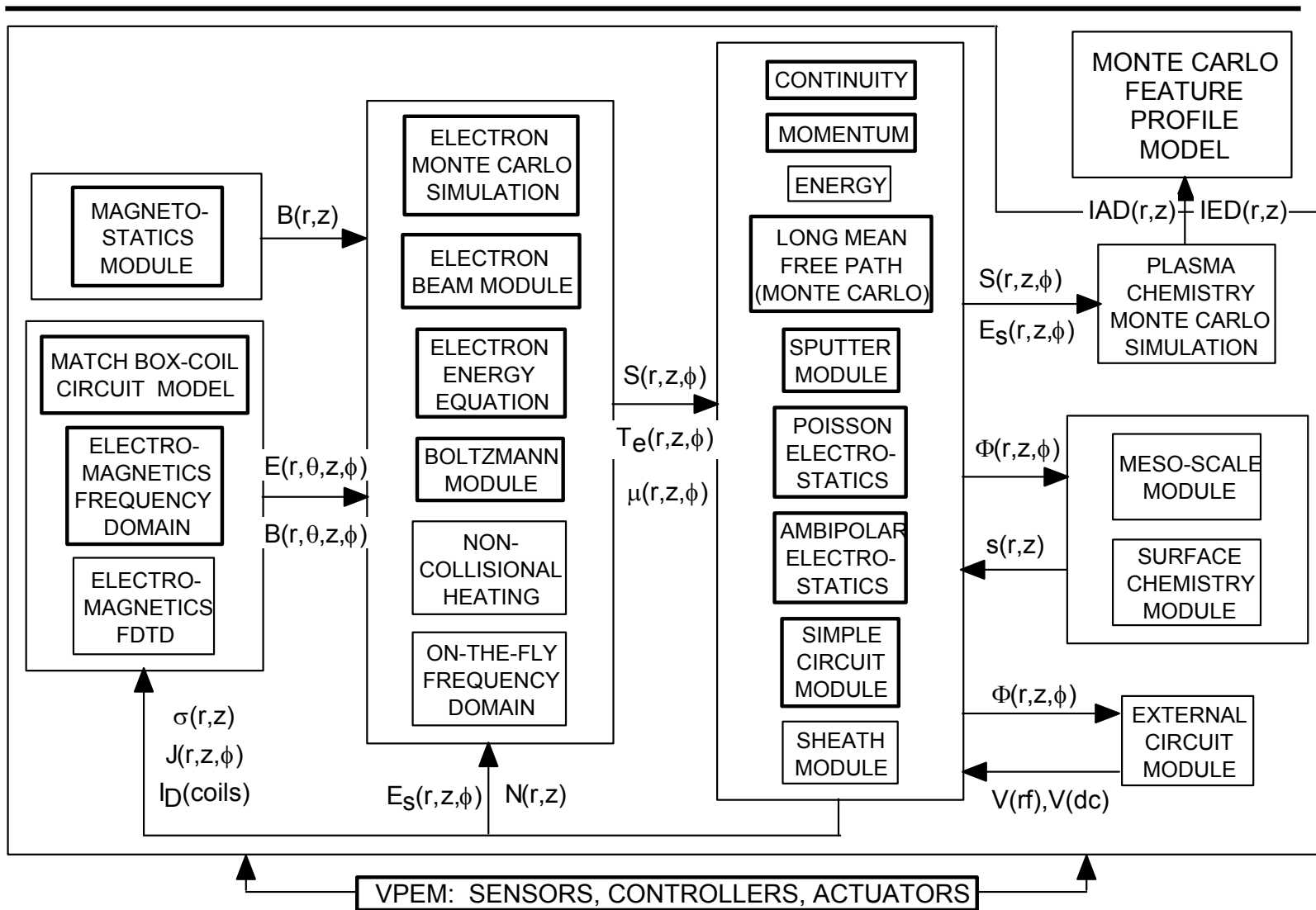
- Owing to the electron energy distribution (EED) is generally non-Maxwellian, a kinetic approach is required for modeling ICPs.

# ELECTRON KINETICS IN ICPs

---

- One of the basic problems in the kinetic simulation of ICPs is the consideration of e-e collisions, which significantly influence the thermal motion of electrons.
- There are at least three approaches to resolve e-e collisions:
  - (i) Particle-in-cell simulations (Nanbu *et al*, 1997, 2000)
  - (ii) Direct solution of Boltzmann's equation (Kolobov *et al*, 1997)
  - (iii) Electron Monte Carlo simulation (Weng *et al*, 1990)

# HYBRID PLASMA EQUIPMENT MODEL



# ALGORITHM FOR E-E COLLISIONS

---

- The basis of the algorithm for e-e collisions is “particle-mesh”.
- Statistics on the EEDs are collected according to spatial location.
- An energy of collision target is randomly selected from the EED at this location

$$P(\varepsilon_{tr}) = f(\varepsilon_{tr})\sqrt{\varepsilon_{tr}}\Delta\varepsilon_{tr}\Delta t / \left( \sum_i f(\varepsilon_i)\sqrt{\varepsilon_i}\Delta\varepsilon_i\Delta t_i \right)$$

- Since, the number of energy bins is usually large (400-500), quick lookup techniques are used for the energy of collision targets.
- In this technique the *l*th cumulative probability is determined from

$$\Pi_l = \sum_{\varepsilon'_{l-1} \leq \varepsilon_j \leq \varepsilon'_l} P(\varepsilon_j) / \sum_i P(\varepsilon_i)$$

# ALGORITHM FOR E-E COLLISIONS

---

- The energy of the collision partner is first randomly selected on a coarse basis, followed by a refinement within the large energy intervals.
- Assuming an isotropic velocity for the target, the probability for an e-e collision is determined using the relative speed between the electron and its target,

$$P_{ee} = n_e(\vec{r}) \cdot \sigma_{ee}(g) \cdot g \cdot \Delta t, \quad g = \left| \vec{v}_{pr} - \vec{v}_{tr} \right|$$

$$\sigma_{ee}(g) = 4\pi b_o^2(g) \left[ 1 + \ln \left( \frac{\lambda_D}{b_o(g)} \right) \right], \quad b_o(g) = \frac{q^2 / 4\pi\epsilon_o}{\frac{1}{2} m_e g^2}$$

# ALGORITHM FOR E-E COLLISIONS

---

- If a collision occurs, then a post collision relative velocity is randomly determined as,

$$g_z' = \pm |\vec{g}| r_1, \quad g_x' = |\vec{g}| \sqrt{1 - r_1^2} \cos(2\pi r_2)$$

$$g_y' = |\vec{g}| \sqrt{1 - r_1^2} \sin(2\pi r_2)$$

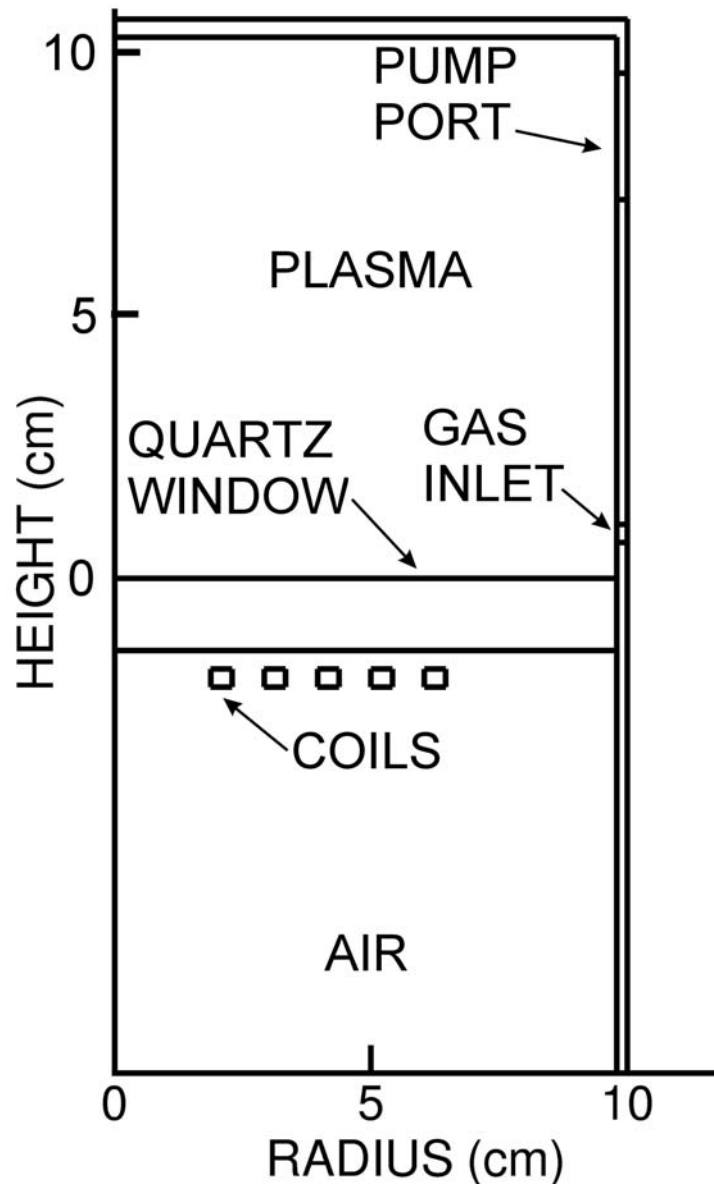
- Finally, the velocity of the pseudo-electron is updated with,

$$\vec{v}_f = \vec{v}_R + 0.5\vec{g}' \quad \vec{v}_R = 0.5(\vec{v}_{tr} + \vec{v}_{pr})$$

- The change in velocity of the collision partner is disregarded; e-e collisions are treated as collisions between pseudo-electrons and energy resolved electron fluid.
- The consequences of e-e collisions on the targets are obtained by continuously updating the stored EEDs.



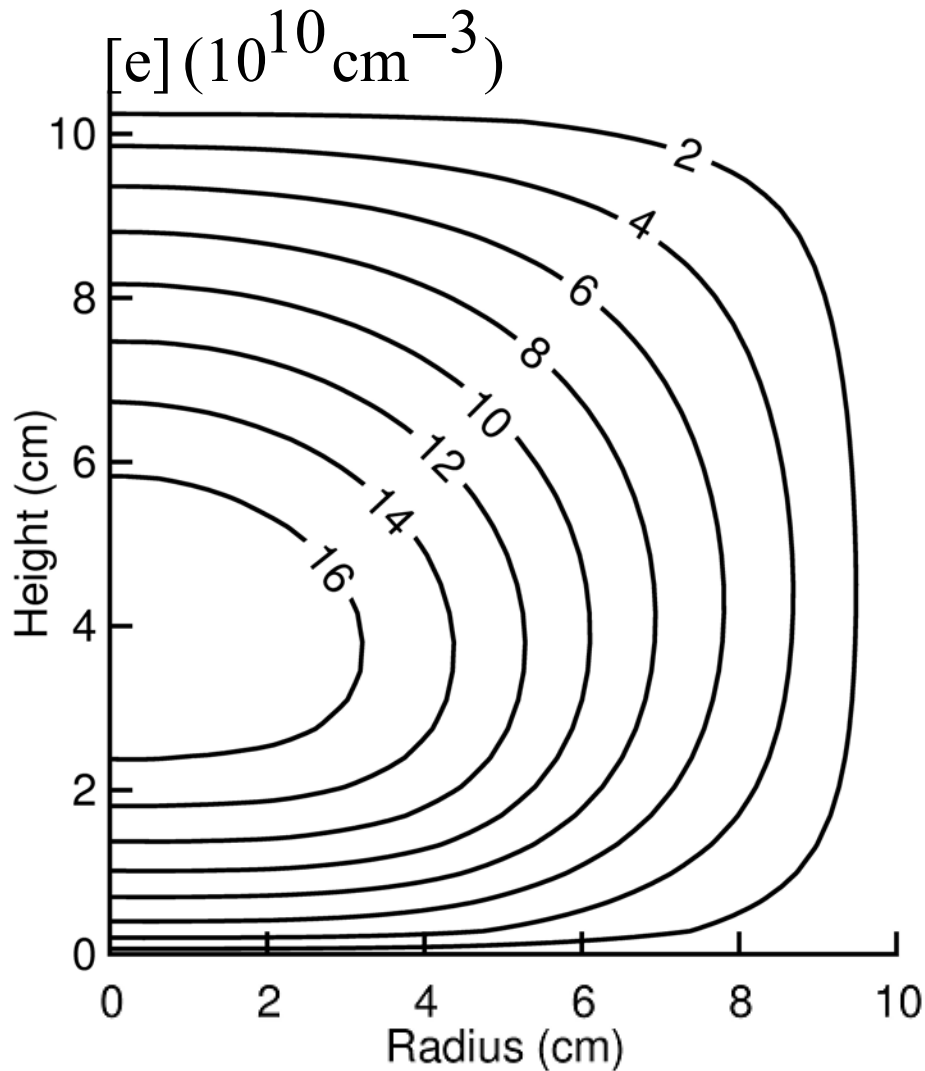
# ICP CELL FOR VALIDATION AND INVESTIGATION



- Experiments by Godyak *et al* (1998) are used for validation.
- The experimental cell is an ICP reactor with a Faraday shield to minimize capacitive coupling.

# ELECTRON DENSITY FOR STANDARD CASE

---

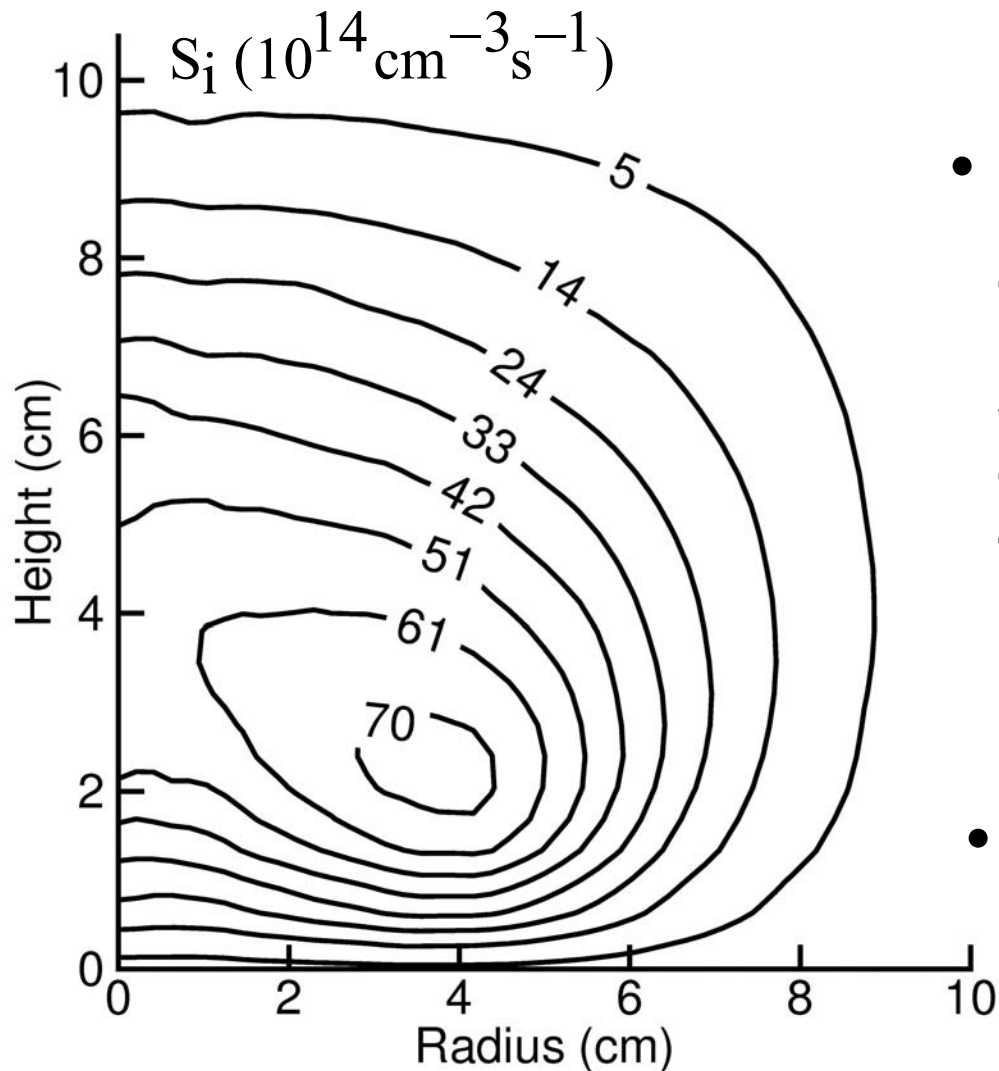


- **Electron density is largest in the middle of reactor where the electric potential is maximum.**

- **Ar, 10 mTorr, 100 W, 6.78 MHz**

# IONIZATION SOURCE FOR STANDARD CASE

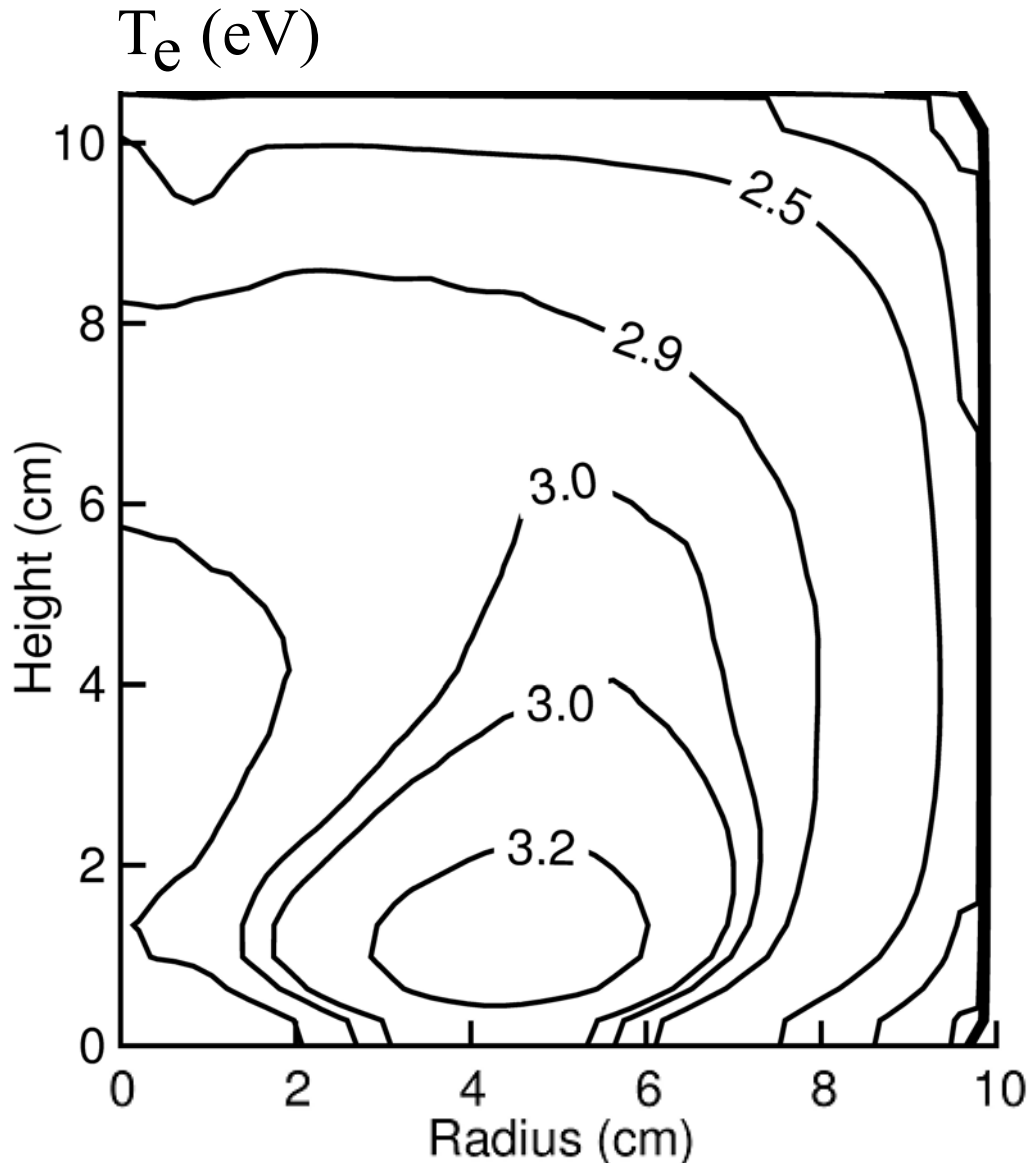
---



- The ionization source reaches a maximum at the edge of the classical skin depth where the amplitude of the electromagnetic field decays to  $1/e$  of its edge value.
- Ar, 10 mTorr, 100 W, 6.78 MHz

# $T_e$ FOR STANDARD CASE: Ar, 10 mTorr, 100 W, 6.78 MHz

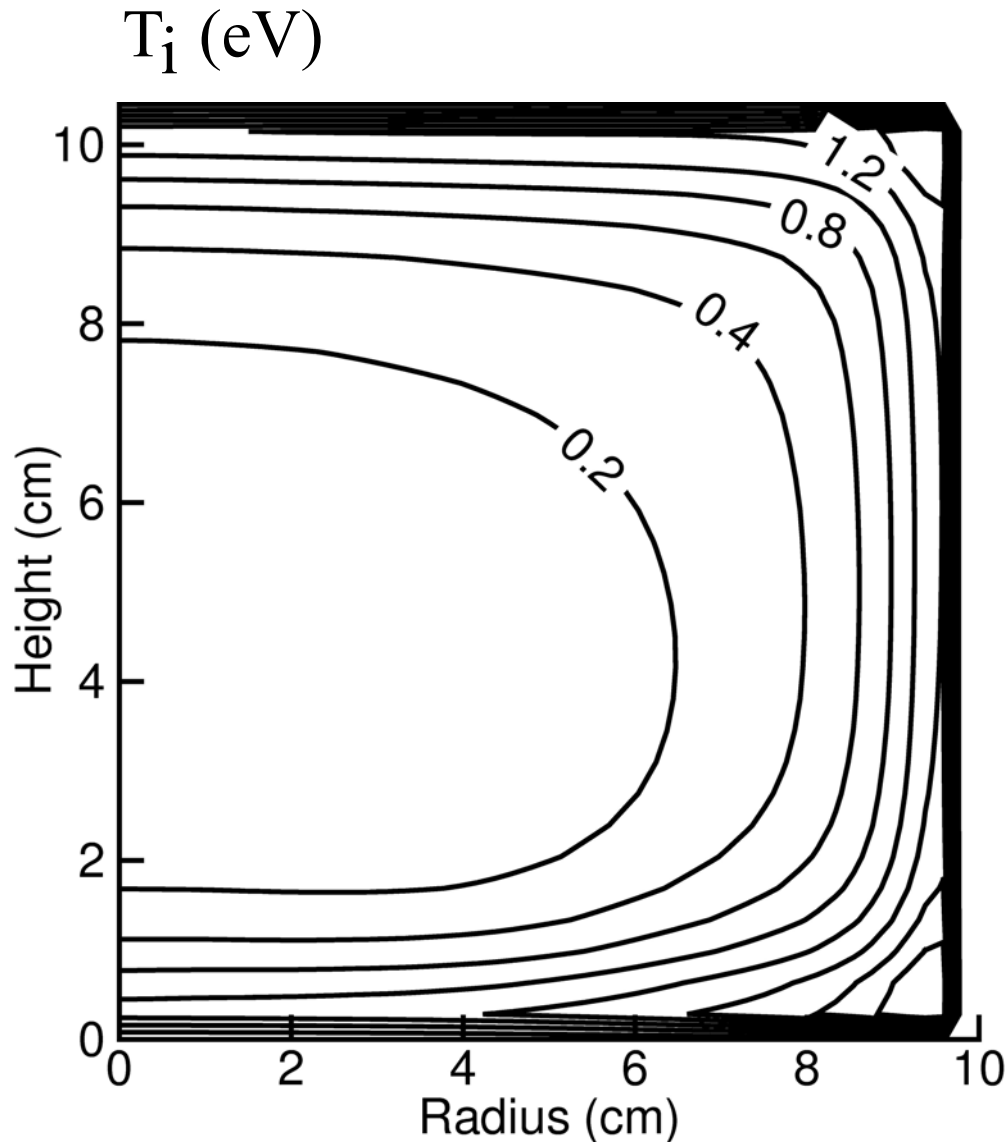
---



- The first major peak occurs in the skin depth owing to collisionless electron heating by the large electric field.
- The second minor peak corresponds to the position where the electron density reaches the maximum.

# $T_i$ FOR STANDARD CASE: Ar, 10 mTorr, 100 W, 6.78 MHz

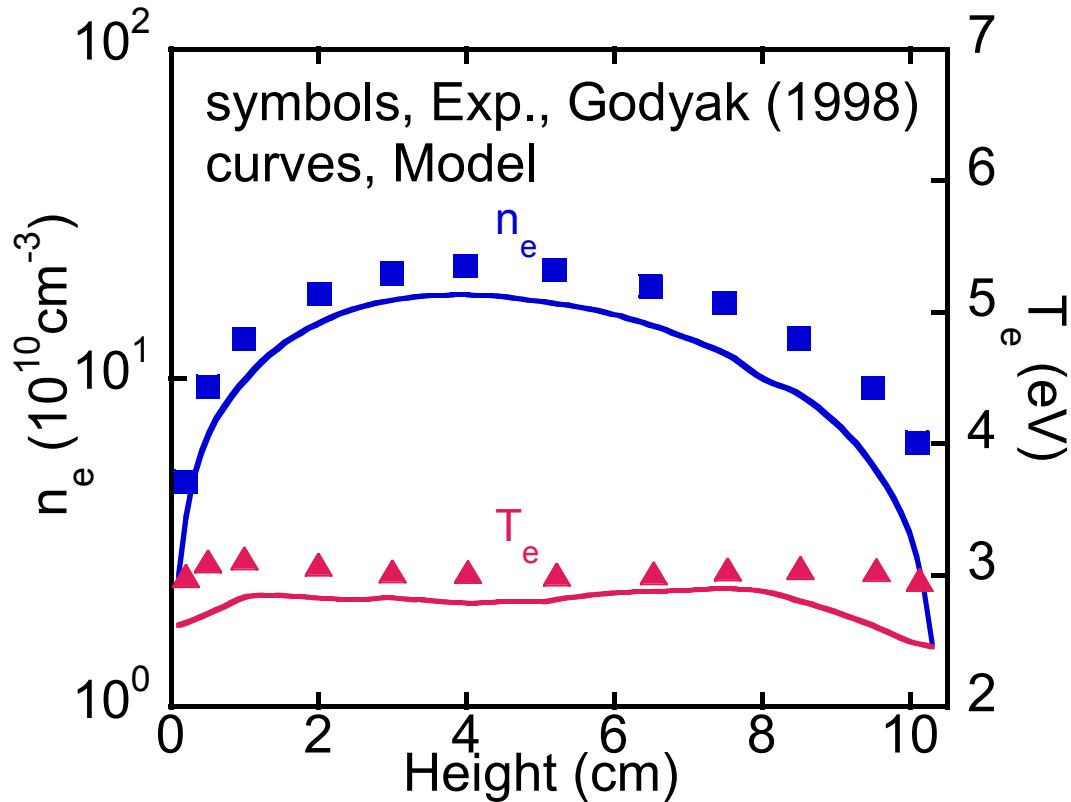
---



- The ion temperature reaches a maximum near the walls where ions gain energy due to acceleration in the presheath.
- In the middle of reactor the ion temperature is lower owing to thermalization with neutral species.

# $T_e$ and $n_e$ ALONG THE CENTERLINE OF THE REACTOR

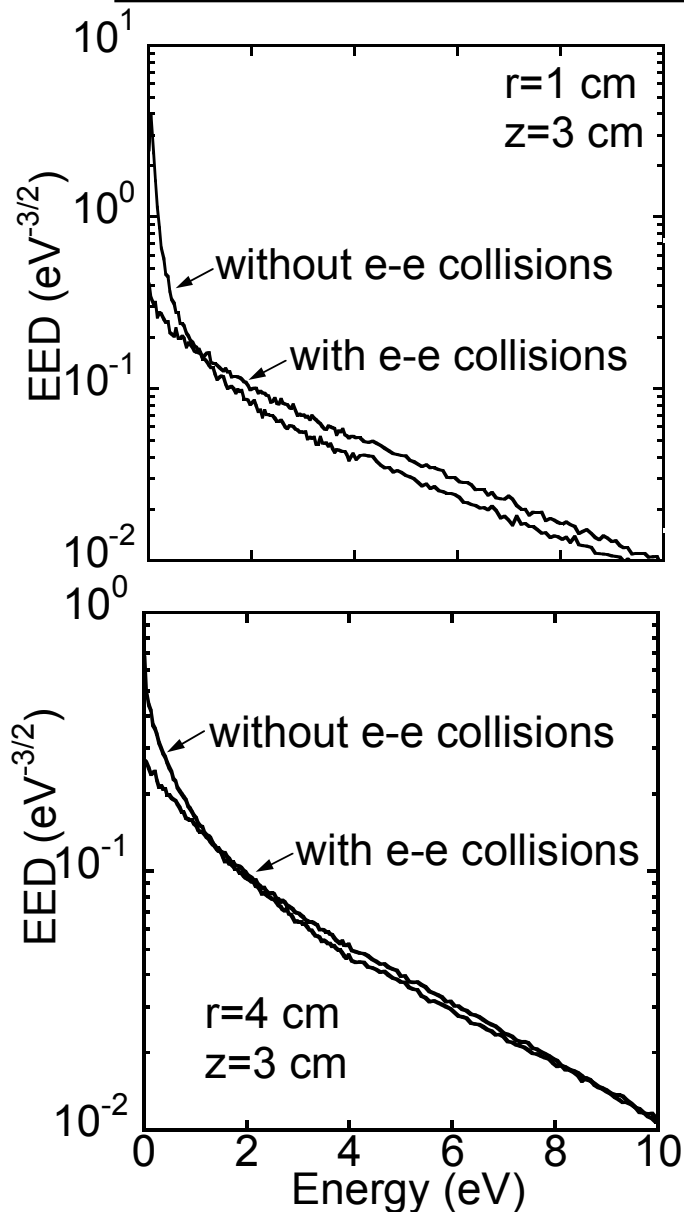
---



- The maximum of electron density is displaced from the center due to the axial location of the source function.
- The high thermal conductivity and redistribution of energy by e-e collisions produce nearly uniform electron temperatures.

- Ar, 10 mTorr, 100 W, 6.78 MHz,  $r=0$

# EFFECT OF E-E COLLISIONS ON THE EEDs

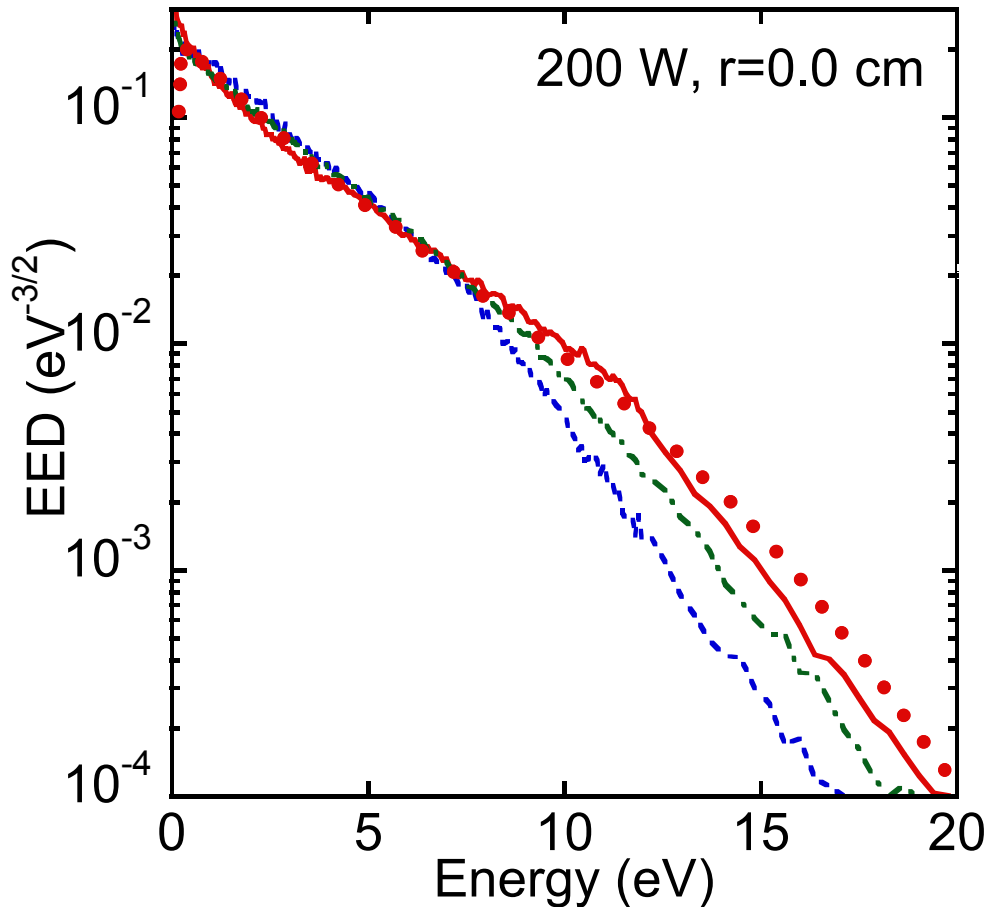


- Low energy electrons want to “pool” at the peak in plasma potential in the center of the reactor.
- When including e-e collisions, the fraction of low-energy electrons is smaller due to energy transfer between low-energy and high-energy electrons.
- Ar, 10 mTorr, 100 W, 6.78 MHz

# EEDs ALONG THE CENTERLINE OF THE REACTOR

---

- Godyak (1998),  $z=5.0$  cm
- Model,  $z=0.5$  cm
- Model,  $z=5.0$  cm
- Model,  $z=10.0$  cm



- Ar, 10 mTorr, 6.78 MHz
- The EEDs show a bi-Maxwellian distribution, which is typical for low-pressure inductively coupled plasmas.
- The EED in the middle of the reactor has the largest energy tail

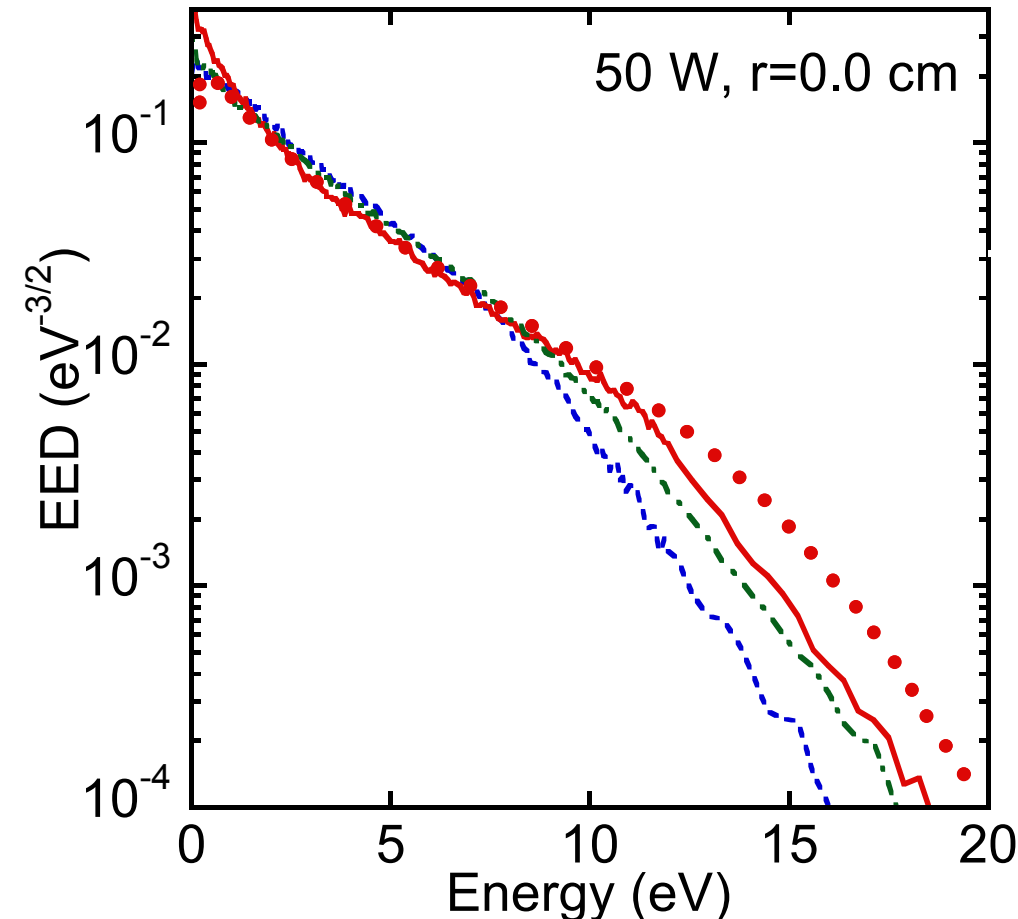


# EEDs ALONG THE CENTERLINE OF THE REACTOR

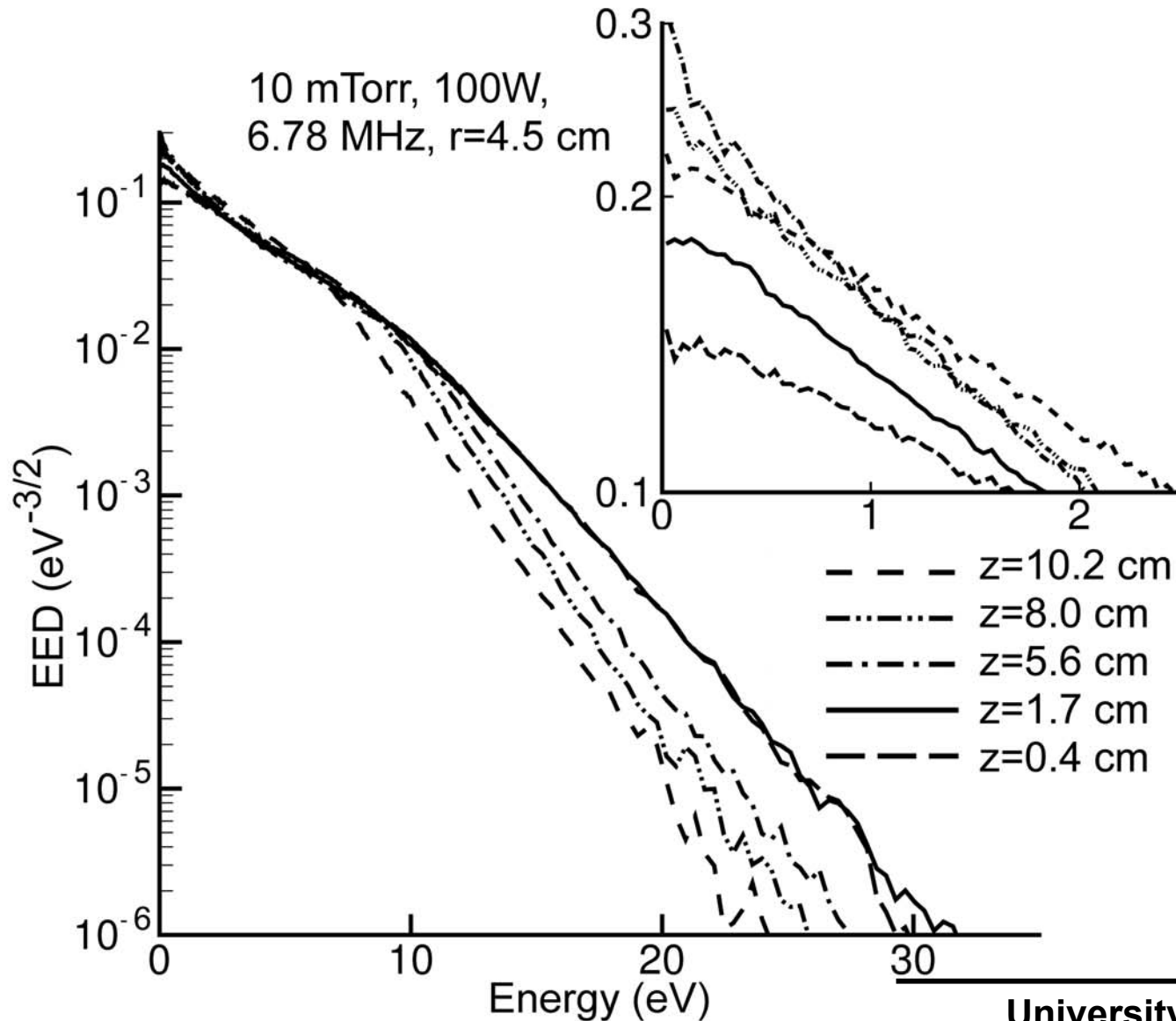
- Godyak (1998),  $z=5.0$  cm
- Model,  $z=0.5$  cm
- Model,  $z=5.0$  cm
- Model,  $z=10.0$  cm

- Ar, 10 mTorr, 6.78 MHz

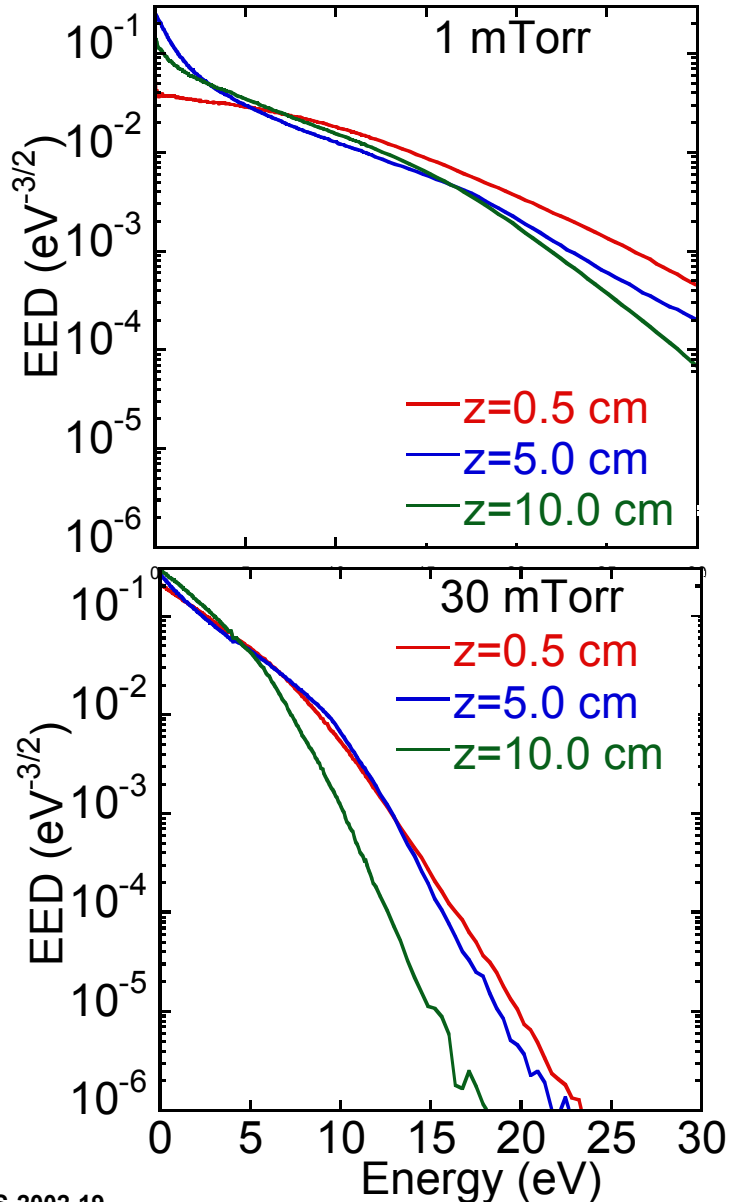
- In the skin layer the EED is depleted at low energies.
- EEDs near the peak plasma potential ( $z = 5.0$  cm) have larger a low energy component.



# EEDs IN SKIN LAYER AND BULK PLASMA

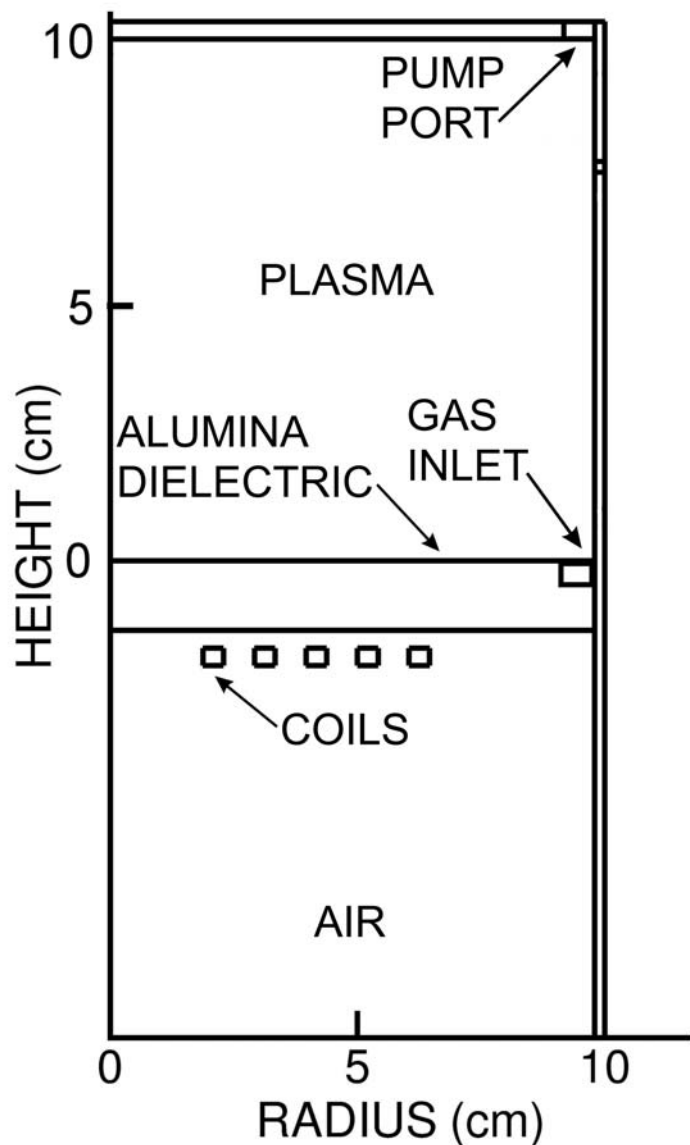


# EFFECT OF PRESSURE ON THE EEDs



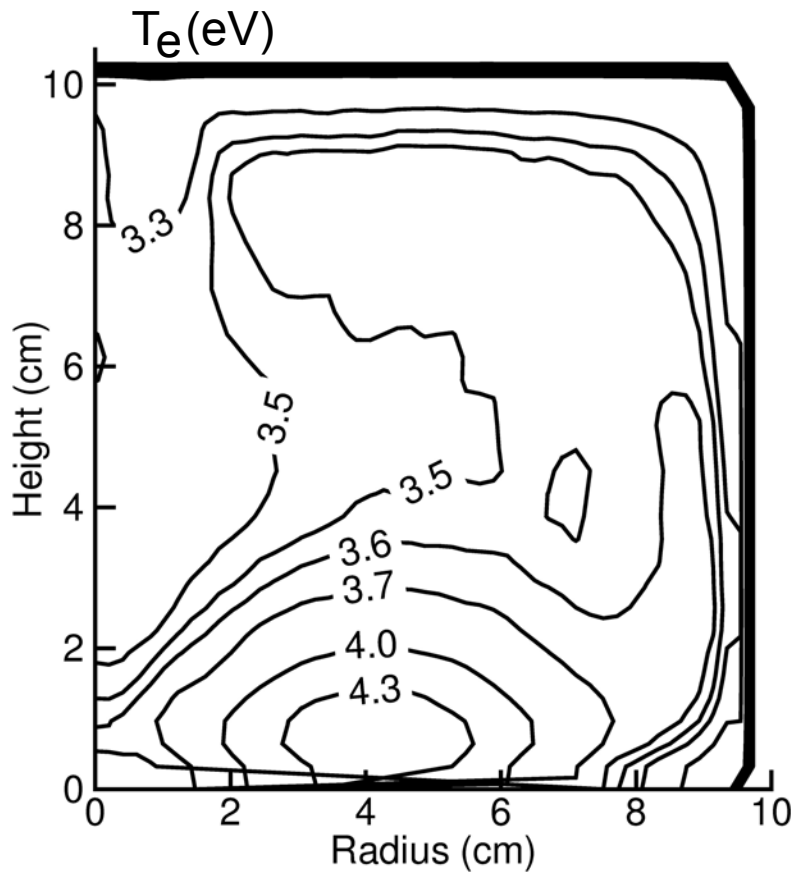
- Ar, 100 W, 6.78 MHz
- At 1 mTorr the EEDs are dominated by collisionless heating and by non-linear Lorentz forces, which provide an axial acceleration.
- The EEDs at 30 mTorr are in a collisional regime and therefore they resemble a Druyvesteyn distribution.

# EXPERIMENTAL CELL FOR INVESTIGATION OF ICPs IN $\text{CF}_4$

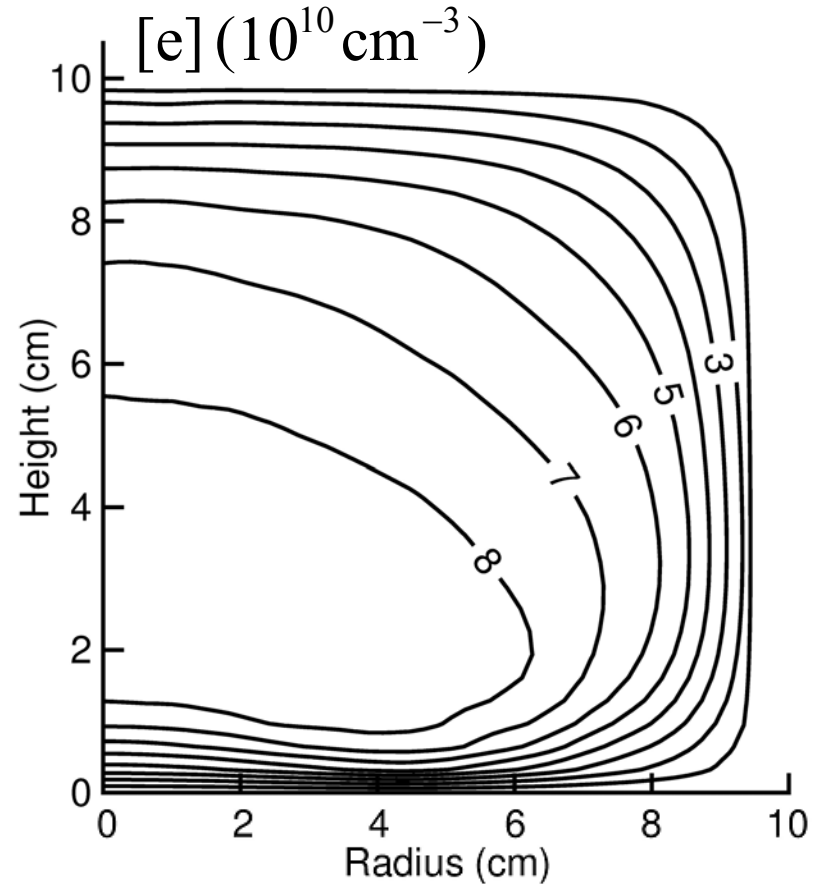


- Modeling of ICPs in  $\text{CF}_4$  involves complex surface and gas-phase chemistry.
- It is particularly challenging due to only limited data is available for electron- $\text{CF}_x$  and  $\text{CF}_x$ - $\text{CF}_x$  radical collisions.
- Experiments by Singh, Coburn, and Graves [J. Vac. Sci. Technol. A v. 19, 718 (2001)] are used for a comparison.

# $T_e, n_e$ for $\text{CF}_4$ , 10 mTorr, 150 W, 13.56 MHz



- **Electron temperature in  $\text{CF}_4$  shows similar features to that in Ar, but it is higher in magnitude due to the dissociation.**



- **The region of largest electron density intersects with the skin layer.**

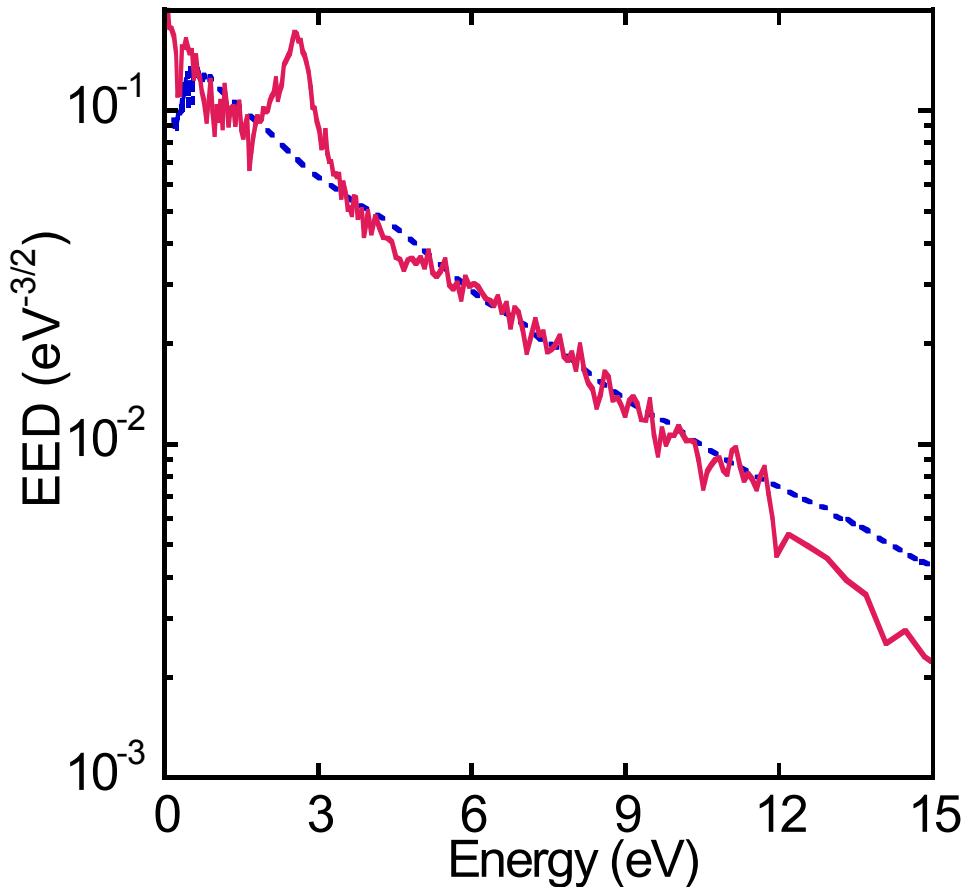
# EXPERIMENTAL AND COMPUTED EEDs

---

----- Exp., Singh et al (2001)      — Model

$n_e = 5 \cdot 10^{10} \text{ cm}^{-3}$

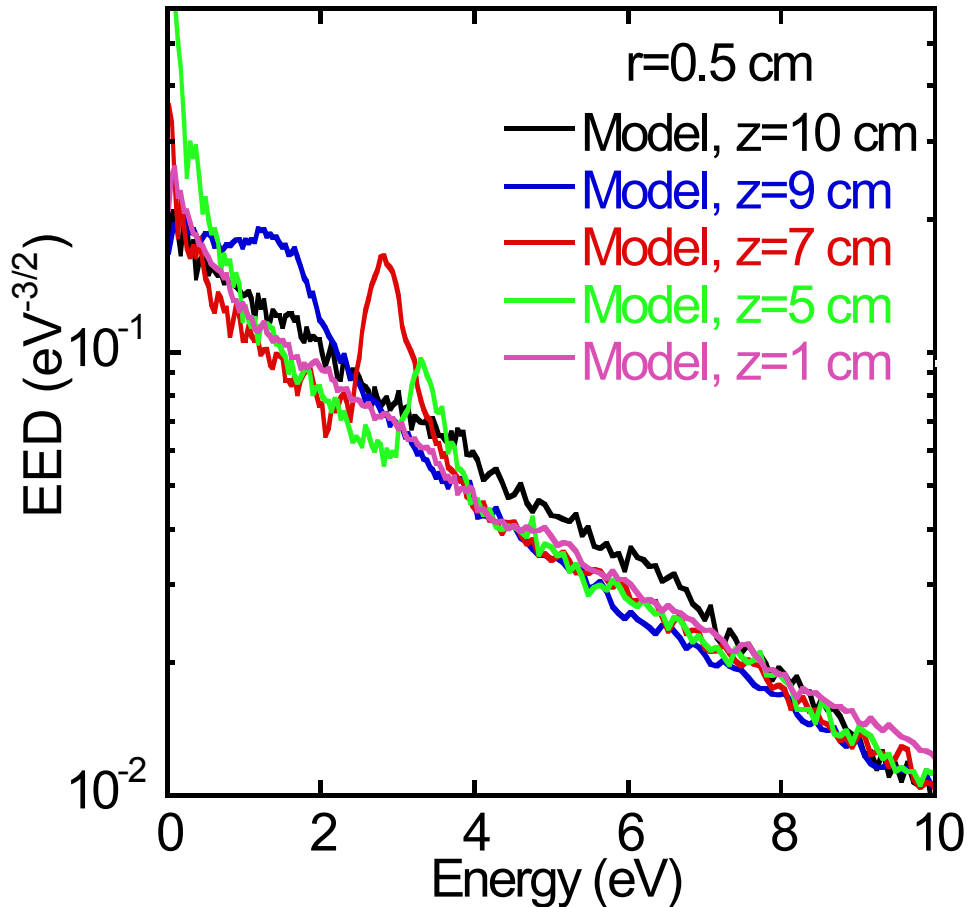
$n_e = 7 \cdot 10^{10} \text{ cm}^{-3}$



- **CF<sub>4</sub>, 10 mTorr, 150 W, 13.56 MHz, r=0, z=7.6 cm**
- **Model yields the same slope as experiment.**
- **A peak in the computed EED occurs at about 3 eV.**

# COMPUTED EEDs IN $\text{CF}_4$ AT DIFFERENT HEIGHTS

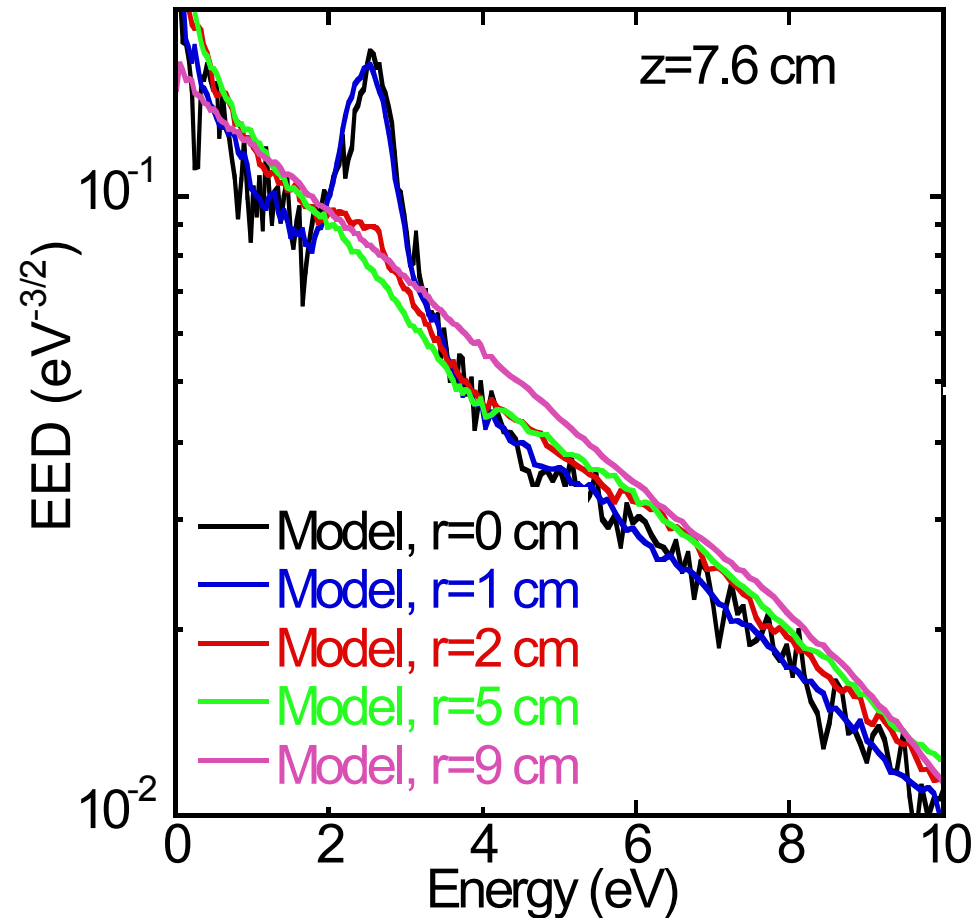
- $\text{CF}_4$ , 10 mTorr, 150 W, 13.56 MHz



- EED is well represented by a Maxwellian distribution in the sheath
- In the bulk plasma the position of the peak shifts to higher energies approaching the skin layer.
- EED in the skin layer shows usual bi-Maxwellian features.

# EDDs IN $\text{CF}_4$ AT DIFFERENT RADII

- $\text{CF}_4$ , 10 mTorr, 150 W, 13.56 MHz

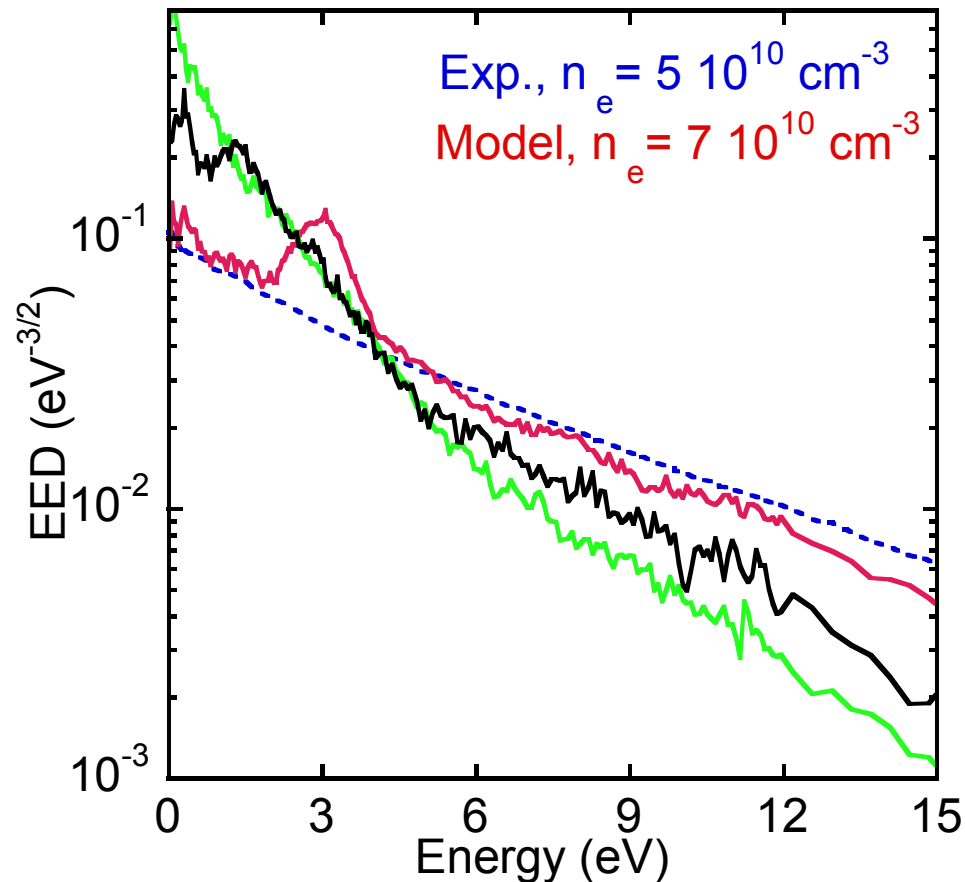


- A peak occurs in the EEDs for radii  $< 2$  cm.
- This peak is formed due to the flux of electrons which collisionlessly propagates from the coils to the opposite wall.
- This flux is formed as a result of interaction between the skin layer and the region of largest electron density.



# EXPERIMENTAL AND COMPUTED EEDs

- Exp., Singh et al (2001)
- Model
- Model, without e-e collisions
- Model, cold plasma



- $\text{CF}_4$ , 3 mTorr, 150 W, 13.56 MHz
- The energy exchange between electrons is eliminated by excluding e-e collisions.
- RF fields do not propagate beyond the normal skin layer when the cold plasma approximation is used.
- In both these cases the thermal electron motion is significantly affected.

# SUMMARY

---

- **We present a new method for modeling e-e collisions in which Coulomb collisions are treated using a test particle approach and, so can be readily included in Monte Carlo simulations of low-pressure and high-density plasma systems.**
- **The method was validated by comparing calculated and measured electron densities, temperatures, and electron distributions in inductively coupled argon plasma.**
- **The EEDs are significantly depleted at low energies in regimes dominated by non-collisional heating.**
- **A maximum in the computed EEDs in  $\text{CF}_4$  depends on the thermal motion of electrons.**

# NET CURRENT FOR CF<sub>4</sub>, 10 mTorr, 150 W, 13.56 MHz

